

Parameterizing redistribution and sublimation of blowing snow for hydrological models: tests in a mountainous subarctic catchment

Matthew K. MacDonald,¹ John W. Pomeroy^{1*} and Alain Pietroniro²

¹ Centre for Hydrology, University of Saskatchewan, Saskatoon, Canada

² National Hydrology Research Centre, Environment Canada, Saskatoon, Canada

Abstract:

Model tests of blowing snow redistribution and sublimation by wind were performed for three winters over a small mountainous sub-Arctic catchment located in the Yukon Territory, Canada, using a physically based blowing snow model. Snow transport fluxes were distributed over multiple hydrological response units (HRUs) using inter-HRU snow redistribution allocation factors (S_R). Three S_R schemes of varying complexity were evaluated. Model results show that end-of-winter snow accumulation can be most accurately simulated using a physically based blowing snow model when S_R values are established when taking into account wind direction and speed and HRU aerodynamic characteristics, along with the spatial arrangement of the HRUs in the catchment. With the knowledge that snow transport scales approximately with the fourth power of wind speed (u^4), S_R values can be (1) established according to the predominant u^4 direction and magnitude over a simulation period or (2) can change at each time step according to a measured wind direction. Unfortunately, wind direction data were available only for one of the three winters, so the latter scheme was tested only once. Although the aforementioned S_R schemes produced different results, model efficiency was of similar merit. The independent effects of topography and vegetation were examined to assess their importance on snow redistribution modelling over mountainous terrain. Snow accumulation was best simulated when including explicit representations of both landscape vegetation (i.e. vegetation height and density) and topography (i.e. wind exposure). There may be inter-basin differences in the relative importance of model representations of topography and vegetation. Copyright © 2009 John Wiley & Sons, Ltd.

KEY WORDS blowing snow; snow transport; sublimation; parameterization; hydrological model; complex terrain

Received 30 June 2008; Accepted 17 April 2009

INTRODUCTION

Snow accumulation over complex arrangements of terrain and vegetation cover such as found in mountains is highly variable due to blowing snow redistribution and other factors. Wind erodes and transports snow from flat surfaces, hilltops, windward slopes and sparsely vegetated surfaces to topographic depressions, leeward slopes and vegetated surfaces. Snow accumulation regimes that vary considerably with topography, vegetation and prevailing wind direction have been observed. Pomeroy *et al.* (1997) found that a total winter snowfall of 190 mm SWE (snow water equivalent) in a low Arctic catchment produced maximum snow accumulations of 68, 252 and 617 mm SWE on tundra, shrub tundra and steep slopes, respectively. McCartney *et al.* (2006) measured maximum seasonal snow accumulations of 102, 229, 164 and 201 mm SWE in short shrub, tall shrub, windward slopes (south-facing) and leeward slopes (north-facing) in a sub-Arctic alpine tundra catchment.

Seasonal snow accumulation governs the magnitude, timing and duration of snowmelt (Luce *et al.*, 1998),

runoff (Anderton *et al.*, 2002) and infiltration of melt-water (Granger *et al.*, 1984). Simulations of snowcover ablation and runoff can be improved by accounting for the effects of landscape heterogeneity on snow accumulation regimes (Déry *et al.*, 2004; Davison *et al.*, 2006; Dornes *et al.*, 2008a).

There has been some success in modelling snow redistribution by wind at point locations, fully distributed (fine) scales and at the landscape scale using physically based and empirical models. Purves *et al.* (1998) developed a rule-based cellular model of snow redistribution based on meteorological, snowpack and terrain variables and applied it over mountainous terrain in Scotland. Pomeroy *et al.* (1997) applied an empirical monthly index blowing snow model to landscape units in the low Arctic, redistributing snow from sparse tundra to shrubs and topographic depressions and hillsides using a source–sink approximation. Winstral *et al.* (2002) developed terrain-based parameters that quantify the effects of complex wind fields on snow distribution patterns. A regression tree model consisting of the terrain-based parameters as well as elevation, solar radiation and slope was used to predict snow depth distribution over alpine terrain using 10 m × 10 m and 30 m × 30 m grids. Winstral's terrain-based parameters were coupled with

* Correspondence to: John W. Pomeroy, Centre for Hydrology, University of Saskatchewan, Saskatoon, Canada.
E-mail: john.pomeroy@usask.ca

a distributed snow model (Winstral and Marks, 2002). These empirical models can provide useful results but are not compatible with physically based hydrological or land surface scheme modelling.

Many physically based blowing snow models are based upon the Prairie Blowing Snow Model (PBSM; Pomeroy, 1989; Pomeroy and Gray, 1990; Pomeroy and Male, 1992; Pomeroy *et al.*, 1993; Pomeroy and Li, 2000). PBSM performs single column mass and energy balance calculations of blowing snow transport and sublimation rates extended to two dimensions using a snow cover mass balance. Essery *et al.* (1999) and Essery and Pomeroy (2004) applied a fully distributed simplified version of PBSM over a low-Arctic tundra catchment using an 80 m × 80 m grid, where snow transport fluxes out of a grid box were directed to an adjacent grid box in one of four directions. Another fully distributed model with similar physics to PBSM, SnowTran-3D (Liston and Sturm, 1998), has been widely applied using grid sizes ranging from 5 m × 5 m to 100 m × 100 m. For instance, SnowTran-3D has been applied over Arctic tundra characterized by gently rolling ridges and valleys (Liston and Sturm, 1998), over mountainous terrain above the tree-line (Greene *et al.*, 1999), over arctic rolling uplands and flat coastal plains (Liston and Sturm, 2002), over gently arching ridges in the treeline zone (Hiemstra *et al.*, 2002) and over glaciated arctic terrain with alpine relief (Hasholt *et al.*, 2003). Spatially aggregated, landscape-based blowing models, wherein snow is relocated from bare and sparsely vegetated surfaces to more densely vegetated and leeward surfaces, have been applied (Pomeroy *et al.*, 1991, 1997; Pomeroy and Li, 2000; Essery and Pomeroy, 2004). Essery and Pomeroy (2004) showed that a spatially aggregated, landscape-based version of PBSM was able to match snow accumulation predicted by a fully distributed version of PBSM reasonably well for a low-Arctic tundra catchment with moderate topography at the catchment scale. Similarly, Fang and Pomeroy (2009) found that fully distributed (6 m × 6 m grid; ~264 000 grid cells) and spatially aggregated (seven landscape units) blowing snow models provided similar simulated snow accumulations to landscape units in a prairie wetland region. Spatially aggregated blowing snow models are much less computationally expensive than fully distributed models.

Many hydrological models and most land surface schemes (LSS) employ some discretization of the landscape into tiles or hydrological response units (HRU). For meso- to macro-scale hydrological applications, these landscape units do not try to capture all of the hydrological variability over a basin, but do capture the major elements of variability due to soil type, vegetation cover, slope, aspect, elevation and position with respect to drainage channels. HRUs can also be defined in aerodynamic terms to be useful for blowing snow modelling (Pomeroy *et al.*, 1997; Essery and Pomeroy, 2004) and can provide a relatively simple way to describe landscape effects on snow redistribution and sublimation processes.

Most macro-scale hydrological models and LSS do not incorporate blowing snow process parameterizations. The authors are aware of only two instances where parameterizations of blowing snow sublimation have been included. Gordon *et al.* (2006) developed a parameterization of blowing snow sublimation for the Canadian Land Surface Scheme (CLASS) by averaging the sublimation rates computed using five existing models. The parameterization, tested at three Canadian sites with different blowing snow event frequencies, improved CLASS snowcover simulations for 23 of 28 winters modelled. Bowling *et al.* (2004) parameterized sub-grid variability in blowing snow sublimation for the VIC (variable infiltration capacity) macro-scale hydrological model. Some of the simulations performed by both Gordon *et al.* (2006) and Bowling *et al.* (2004) could have been improved by including a parameterization of snow transport in addition to the sublimation calculations. For instance, as wind-eroded snow from upwind HRUs is deposited into a heavily vegetated HRU, both snow accumulation and the effective fetch increase, resulting in greater blowing snow sublimation (Bowling *et al.*, 2004).

OBJECTIVES

The purpose of this study is to convey information regarding the level of parameterization complexity that is required to simulate snow redistribution in mountain topography at the basin scale. The objectives of this paper are to

1. simulate end-of-winter snow accumulation in HRUs over a small mountainous subarctic tundra catchment using a physically based blowing snow model;
2. compare and assess the effectiveness of landscape- and meteorology-based parameterizations of snow redistribution of varying levels of complexity; and
3. evaluate the effects of topography and vegetation parameterizations on the accuracy of the blowing snow simulations.

STUDY SITE

The study site is the Granger Basin (GB; 60°31'N, 135°07'W; 1310–2100 m asl), an 8 km² sub-basin of the Wolf Creek Research Basin (WCRB), located approximately 15 km south of Whitehorse, Yukon Territory, Canada (Figure 1, inset). WCRB is part of the headwater region of the Yukon River Basin. Climate normals (1971–2000) for the Whitehorse International Airport (WIA; 60°42'N, 135°04'W; 706 m asl) specify a daily average temperature of −0.7 °C on an annual basis, with January (coldest month) and July (warmest month) having daily average temperatures of −17.7 and 14.1 °C, respectively. The mean annual precipitation at the WIA is 267 mm with approximately half as snowfall, though Pomeroy *et al.* (1999) show that precipitation is 25 to 35% greater over WCRB and that the fraction that is

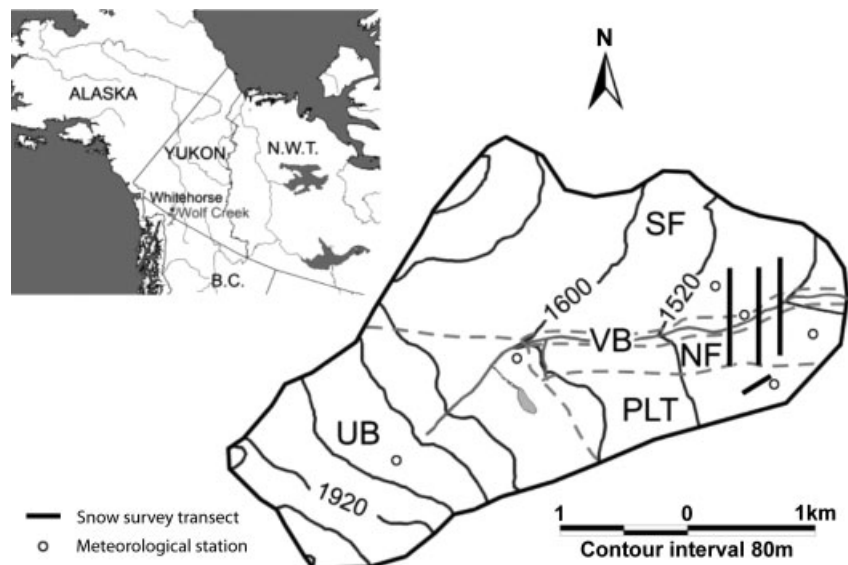


Figure 1. Wolf Creek Research Basin location (inset), Granger Basin HRUs. UB, upper basin; PLT, plateau; VB, valley bottom; NF, north-facing slope; SF, south-facing slope (Reproduced and by permission from Dornes *et al.* (2008a))

snowfall is higher, mainly due to the elevation difference. There are 71 days per annum with snowfall at WIA, though likely more over WCRB. The snowfall regime of WCRB is typical of the northern boreal cordillera of Western Canada (Pomeroy *et al.*, 1999). The annual average relative humidity (RH) at 0600 and 1500 local standard time (LST) is 74 and 55%, respectively.

GB landcover at high elevations consists of exposed mineral soils and sparse grasses, lichens and mosses. At intermediate elevations, mineral soils are more densely covered by short shrubs. At low elevations, tall shrubs cover a relatively wetter surface layer. A surface organic layer up to 0.4 m thick is present in permafrost and low elevations areas (Carey and Quinton, 2004).

MODELLING METHODOLOGY

Prairie blowing snow model (PBSM)

PBSM was used to simulate blowing snow transport, sublimation and the resulting snow accumulation over GB. PBSM does this by calculating two-dimensional blowing snow transport and sublimation rates for steady-state conditions over a landscape using mass and energy balances. PBSM was initially developed for application over the Canadian Prairies, which are characterized by relatively flat terrain and homogeneous crop cover (e.g. Pomeroy, 1989; Pomeroy *et al.*, 1993). Versions have been applied to variable vegetation height (Pomeroy *et al.*, 1991) over alpine tundra (Pomeroy, 1991) and arctic tundra (Pomeroy and Li, 2000). Only key equations are presented here. Refer to Pomeroy *et al.* (1993) and Pomeroy and Li (2000) for a more complete description of PBSM.

The snow mass balance over a uniform element of a landscape (e.g. an HRU) is a result of snowfall accumulation and the distribution and divergence of

blowing snow fluxes both within and surrounding the element given by

$$\frac{dS}{dt}(x) = P - p \left[\nabla F(x) + \frac{\int E_B(x) dx}{x} \right] - E - M \quad (1)$$

where dS/dt is surface snow accumulation ($\text{kg m}^{-2} \text{s}^{-1}$), P is snowfall ($\text{kg m}^{-2} \text{s}^{-1}$), p is the probability of blowing snow occurrence, F is the snow transport rate ($\text{kg m}^{-1} \text{s}^{-1}$), E_B is blowing snow sublimation ($\text{kg m}^{-2} \text{s}^{-1}$), x is fetch (m), E is the snow surface sublimation ($\text{kg m}^{-2} \text{s}^{-1}$) and M is snow melt ($\text{kg m}^{-2} \text{s}^{-1}$). During winter in cold environments when blowing snow events occur relatively frequently, M is relatively small and it is considered negligible during the Yukon winter.

Blowing snow fluxes are the sum of snow transport in the saltation and suspension layers, F_{salt} and F_{susp} ($\text{kg m}^{-1} \text{s}^{-1}$), respectively. Saltation of snow must be initiated before snow transport can occur in the suspension layer and blowing snow sublimation can occur.

F_{salt} is calculated using a shear stress partitioning as presented by Pomeroy and Gray (1990):

$$F_{\text{salt}} = \frac{c_1 e \rho u_t^*}{g} (u^{*2} - u_n^{*2} - u_t^{*2}) \quad (2)$$

where c_1 is the dimensionless ratio of saltation velocity to friction velocity ($u_p/u^* = 2.8$), e is the dimensionless efficiency of saltation ($1/4.2 u^*$), ρ is atmospheric density (kg m^{-3}), g is acceleration due to gravity (m s^{-2}), u^* is the atmospheric friction velocity (m s^{-1}), and u_n^* and u_t^* refer to the portions of the u^* applied to non-erodible roughness elements such as vegetation (non-erodible friction velocity) and the open snow surface itself (threshold friction velocity), respectively. u_t^* is calculated from the meteorological history of the snowpack using an algorithm developed by Li and Pomeroy (1997).

u_n^* is calculated using an algorithm developed by Raupach *et al.* (1993) for wind erosion of soil calculations that relates the partitioning of the shear stress to the geometry and density roughness elements given by

$$\frac{u_n^*}{u^*} = \frac{(m \beta \lambda)^{0.5}}{(1 + m \beta \lambda)^{0.5}} \quad (3)$$

where β is the ratio of element to surface drag and λ is the dimensionless roughness element density. Raupach *et al.* (1993) found $\beta \approx 170$ which is used in PBSM for blowing snow simulation of short grass and crop stalks. m is an empirical constant to account for the difference in average and maximum surface shear stress to initiate erosion. The default value for m in PBSM is 1.0. Wyatt and Nickling (1997) determined a mean $\beta = 202$ and a mean $m = 0.16$ for desert creosote shrubs (*Larrea tridentata*) in a Nevada desert. Wyatt and Nickling's β and m are presumed to be more suitable for shrubs in GB than the grass and cereal grain default values in PBSM. λ is calculated as per Pomeroy and Li's (2000) modification of an original equation by Lettau (1969):

$$\lambda = Nd_v \left(h_v - \frac{S}{\rho_s} \right) \quad (4)$$

where N is the vegetation number density (number m^{-2}), d_v is the vegetation stalk diameter (m), h_v is the height of vegetation and the snow depth is snow accumulation S divided by snow density ($kg\ m^{-3}$).

F_{susp} is calculated as a vertical integration from a reference height near the top of the saltation layer h^* to the top of blowing snow boundary layer (z_b), given by Pomeroy and Male (1992):

$$F_{susp} = \frac{u^*}{k} \int_{h^*}^{z_b} \eta(z) \ln \left(\frac{z}{z_0} \right) dz \quad (5)$$

where k is von Kármán's constant (0.41), η is the mass concentration of blowing snow at height z (m) and z_0 is the aerodynamic roughness height. z_b is governed by the time available for the vertical diffusion of snow particles from h^* , calculated using turbulent diffusion theory and the logarithmic wind profile. For fully developed flow, it is constrained as $z_b = 5$ m. At z_b , shear stress is constant ($d\tau/dt = 0$) and suspension occurs under steady-state conditions ($d\eta/dt = 0$). Note that as suspension diffuses from the saltation layer, saltation must be active for suspension to proceed.

E_B is calculated as a vertical integration of the sublimation rate of a single ice particle with mean mass described by a two-parameter gamma distribution of particle size that varies with height, as given by Pomeroy *et al.* (1993):

$$E_B = \int_0^{z_b} \frac{1}{m(z)} \frac{dm}{dt}(z) \eta(z) dz \quad (6)$$

where m is the mean mass of a single ice particle at height z . The rate at which water vapour can be removed from the ice particle's surface layer dm/dt is calculated

as a balance of radiative energy exchange, turbulent convective heat transfer and latent heat exchange during phase change, assuming that snow particles remain in thermodynamic equilibrium. dm/dt is also controlled by the radius of the ice sphere, the diffusivity of water vapour in the atmosphere, the degree of turbulent transfer of water vapour from the particle surface to the air and the water vapour density of both the ambient air and the particle surface. E_b calculations are highly sensitive to ambient RH, temperature and wind speed (Pomeroy *et al.*, 1993; Pomeroy and Li, 2000).

Inter-HRU snow redistribution allocation factor

Simulating snow redistribution over a catchment with multiple HRUs can be accomplished using snow redistribution allocation factors (S_R). The S_R specifies the fraction of snow transport that is transported from upwind HRUs to a given downwind HRU as opposed to other downwind HRUs. At each model time step, the sum of the snow transport from all HRUs is summed. This total snow transport is distributed to HRUs using the pre-determined S_{RS} . The total snow transport from all HRUs is distributed rather than separately distributing the snow transport from individual HRUs because during blowing snow events, a steady-state flow condition can develop across an aggregated fetch composed of multiple HRUs. Snow transport is allowed to enter a catchment via the most upwind HRU (HRU 1) according to the modelled HRU 1 snow transport and the S_R specified for basin gain (i.e. snow transport into catchment is distributed only to HRU 1 and is equal to $S_{R,gain} \cdot p_1 \cdot (F_{salt,1} + F_{susp,1})/x_1$) where the subscript 1 denotes snow transport terms for HRU 1. Snow transport is also allowed to leave the catchment according to $S_{R,basin\ loss}$. Hence, the number of S_{RS} is equal to $n + 1$, where n is the number of HRUs.

Inclusion of inter-HRU snow transport in the snow mass balance over an HRU results in a discretization of the divergence of transport rates in Equation (1). The snow mass balance over an HRU j that receives snow transport from other HRUs is therefore given by a modification of Equation (1):

$$\begin{aligned} \frac{dS_j}{dt}(x) = & P_j + S_{R,j} \sum [p_i \cdot \nabla F_i(x)] \\ & - p_j \left[\nabla F_j(x) + \frac{\int E_{B,j}(x) dx}{x_j} \right] \\ & - E_j - M_j \end{aligned} \quad (7)$$

where $S_{R,j}$ is the snow redistribution allocation factor for HRU j .

Three S_R schemes were evaluated for this paper:

1. all HRUs receive the same amount of snow transport (all S_{RS} equal);
2. S_{RS} are assigned to HRUs considering the predominant seasonal measured wind direction(s), HRU aerodynamic and topographic characteristics and the spatial arrangement of HRUs;

3. S_{RS} are binned by wind direction considering the spatial arrangement of HRUs and therefore can change with each time step. Eight binned directions were used (the four cardinal and the four primary inter-cardinal directions).

For S_R Scheme 1, all S_{RS} (including $S_{R, \text{basin loss}}$) are equivalent. S_R Scheme 1 is the most rudimentary approach to inter-HRU snow redistribution. Its application disregards the direction of blowing snow events, HRU aerodynamic characteristics that govern snow erosion rates as well the proximity and size of HRUs.

Application of S_R Schemes 2 and 3 requires wind direction and speed data and a pre-established spatial arrangement of the HRUs. First, it must be determined which HRUs are sources and which are sinks of snow transport (resulting in positive and negative snow erosion rates, respectively). This is accomplished by simulating snow transport fluxes in the point mode for each HRU using PBSM. When HRUs are selected based upon the characteristics that govern snow accumulation (i.e. wind exposure and aerodynamic roughness), it is usual that snow transport source and sink HRUs can be distinctly identified. Schemes 2 and 3 S_{RS} were parameterized using interface lengths d between source and sink HRUs perpendicular to the wind direction. Pomeroy and Male (1992) showed that snow transport fluxes scale approximately with the fourth power of wind speed (u^4). Essery *et al.* (1999) used this expression to parameterize a simplified version of PBSM. For S_R Scheme 2, the predominant u^4 resultant direction over a winter is used to determine the interface lengths d_i between source and sink HRUs. Therefore, S_R Scheme 2 assumes that all snow transport occurs in the predominant u^4 resultant direction. For S_R Scheme 3, the wind direction at each time step is used to determine d_i . An illustration of the d_i concept is shown on Figure 3 for GB. The S_R parameterization presumes that all snow transported from source to sink HRUs occurs across and perpendicular to d_i . The S_R for snow transported to HRU j is given by

$$S_{R,j} = L_{C,j} \frac{d_j}{\sum d_i} \quad (8a)$$

for sink HRUs adjacent to source HRUs, and by

$$S_{R,j} = (1 - L_{C,k}) \frac{d_k}{\sum d_i} \quad (8b)$$

for sink HRUs not adjacent to sources HRUs. d_j is the length of the interface between source HRUs and HRU j perpendicular to the predominant u^4 (or wind) direction, and d_i is the length of the interface between source HRUs and all sink HRUs i to which snow is transported, perpendicular to the predominant u^4 (or wind) direction. d_k is the interface length between source HRUs and HRU k that is upwind of HRU j which is adjacent to source HRUs. L_C is a fractional term to account for the 'snow trapping efficiency' of a leeward slope HRU.

Over hilly and mountainous terrains, snow can be transported from an upwind HRU and deposited into a downwind HRU that is not directly adjacent to the upwind HRU. For instance, snow can be transported from over a leeward slope and deposited in a downwind valley bottom. A leeward slope represents an increase in landscape aerodynamic roughness that reduces the downwind boundary layer wind speed. If the step change in elevation and slope is sufficient, a positive snow erosion regime can abruptly become negative causing deposition of snow; this often happens when flow enters a leeward slope. The decay in the horizontal flux of snow transport from this 'boundary' of positive/negative snow erosion rates can be used to estimate the fraction of snow transport that is deposited into a leeward slope as opposed to a downwind valley bottom. Unfortunately, observations of changes in snow transport rate in response to a step decrease in wind speed are lacking. Takeuchi (1980) measured the downwind increase in the horizontal flux of snow transport from a wooded boundary. Results were presented for various snow transport threshold conditions and wind speeds at a vertical scale of 0.3 m. A hyperbolic increase in snow transport rate was observed until fully developed flow was established from 200 to 300 m downwind from the wooded boundary. To the authors' knowledge, Takeuchi's measurements remain the best field measurements of the horizontal development of snow transport rates. The fraction of snow transport that is deposited into a leeward slope as opposed to a downwind valley bottom can be estimated presuming that the decrease in the horizontal flux of snow transport follows the same profile as the increase in the horizontal flux as measured by Takeuchi. Pomeroy and Male (1986) developed a hyperbolic function that approximates the shape of Takeuchi's horizontal profiles given by

$$L_C = \frac{\tanh\left(4\frac{L}{300} - 2\right)}{2} + 0.5 \quad (9)$$

where L_C is the horizontal mass flux as a fraction of the fully developed flux at L , the distance downwind from an aerodynamic barrier (m). The distance required to attain fully developed flow was taken to be Takeuchi's upper value of 300 m, since measurements were limited to a vertical scale of 0.3 m. Equation (9) yields $L_C = 0.07$ at $L = 50$ m, $L_C = 0.50$ at $L = 150$ m and $L_C = 0.98$ at $L = 300$ m.

In the proposed method, L_C is the parameterization of the fraction of snow transport that is deposited into a leeward slope HRU and $1 - L_C$ is the fraction of snow transport that is deposited into the adjacent downwind HRU, such as a valley bottom. This method assumes that the snow transport regime upwind of the leeward slope HRU is fully developed and that a negligible quantity of snow is eroded from the leeward slope and thus all airborne snow particles above a leeward slope are a result of snow transport from an upwind location or from snowfall. Flow separation over the crest of a leeward slope is not accounted for. Equation (9) is independent

Table I. Granger Basin HRUs physiographic characteristics

HRU	Area (km ²)	Elevation range (m ASL)	Vegetation cover	Vegetation height (m)	Vegetation diameter (m)	Vegetation density (number m ⁻²)	Fetch ^c (m)
UB	3.1	1600–2100	Bare ground and rocks	0.10 ^a	0.1 ^a	0.5	734
PLT	0.8	1460–1520	Short shrubs	0.3	0.3	1	319
NF	0.6	1350–1460	Mixed shrubs	0.69–0.79 ^b	0.8	1	300 ^d
SF	3.2	1350–1760	Mixed shrubs	0.69–0.79 ^b	0.8	1	631
VB	0.3	1310–1350	Tall shrubs	1.3–1.4 ^b	0.8	1	300 ^a

^a 0.10 m vegetation height and diameter were used to simulate the roughness effect of sparse vegetation and rocks.

^b Vegetation height was assumed to increase by 2 cm year⁻¹. Vegetation height set based on 2008 measurements along snow survey transects.

^c Average of northwest and southwest fetch distances.

^d Set to 300 m because measured fetch distance was less than minimum required by PBSM (300 m).

of wind speed, and turbulent effects on snow particle vertical velocity are ignored.

GRANGER BASIN MODEL PARAMETERIZATION

HRU selection

A landscape-based aggregated approach rather than a fully distributed fine-scale approach was employed. Five HRUs were used to simulate snow redistribution over GB (Figure 1, Table I): Upper Basin (UB), Plateau (PLT), North-facing slope (NF), South-facing slope (SF) and Valley Bottom (VB). These five HRUs were selected for hydrological modelling based on field observations of sun and wind exposure, slope, vegetation cover and soil type (McCartney *et al.*, 2006), usefulness in snow hydrology modelling (Dornes *et al.*, 2008a) and careful consideration of the landscape features that govern snow accumulation and redistribution (Pomeroy *et al.*, 1999, 2006). The HRUs were delineated as per Dornes *et al.* (2008a). Dornes *et al.* (2008a,b) determined that these five HRUs are adequate for accurately simulating snow-cover ablation and runoff at GB; hence, a consequential objective of this paper is to determine whether HRUs delineated for modelling the hydrology of the snowmelt period are also suitable for modelling winter snow accumulation. Certainly the characteristics that control the snow accumulation available for melt are extremely important for both accumulation and melt calculations.

Field measurements

Simulations were performed for October through April 1998/1999, 2000/2001 and 2003/2004 over GB. Meteorological observations from five meteorological stations located at GB were used. All simulations were performed at 1-h intervals. The meteorological stations were located on all five HRUs (Figure 1). The PLT meteorological station data was available only for 2003/2004. PLT was driven by UB wind speed, and NF RH and temperature for 1998/1999 and 2000/2001. Since the UB meteorological station was not installed until April 1999, regression relationships of UB meteorological observations to SF meteorological observations were used to create synthetic data for UB from October 1998 to March 1999.

Daily precipitation was not measured at WCRB over the study periods; therefore precipitation data from the WIA Nipher-shielded snow gauge were used. Precipitation measurements were corrected for wind effects, wetting losses and unrecorded trace events using the correction procedure recommended by Goodison *et al.* (1998). WIA precipitation measurements had to be increased for application over GB, due to the elevation difference-induced greater precipitation over WCRB than over WIA (Pomeroy *et al.*, 1999). Observations of end-of-winter snow accumulation in non-windswept areas at various elevations of WCRB during winters 1993/1994, 1994/1995 and 1996/1997 were used to generate multipliers which ranged from 1.09 to 1.70 to extrapolate precipitation from the WIA to each GB HRU. The mean of the precipitation multipliers generated for all three winters (1.31 to 1.41 depending on HRU elevation) was applied to the WIA precipitation measurements to extrapolate WIA precipitation measurements to GB HRUs. This mean precipitation multiplier proved to be adequate for simulating GB snow redistribution for 1998/1999 and 2000/2001 when compared to GB snow surveys. For 2003/2004, however, GB snow accumulation was severely overestimated over each HRU, suggesting that the mean multiplier was unrealistic in that season. For that reason, the lowest measured seasonal precipitation multiplier (1.09 to 1.12 depending on HRU elevation) was applied to WIA precipitation measurements for 2003/2004 simulations. The multipliers generated are consistent with observed increase in snow accumulation over certain mountains in the British Columbia Rocky Mountains (Auld, 1995) and analysis of WCRB-corrected snowfall by Pomeroy *et al.* (1999). Table II presents total precipitation, mean temperature, mean RH and mean wind speed for each HRU for each simulation period. Meteorological observations were similar from year to year. Total precipitation was greatest over 1998/1999 and lowest over 2000/2001. Wind speed, from highest to lowest, was UB/PLT, SF, NF and VB, for each simulation period.

Snow surveys that span the NF, SF and VB HRUs (Figure 1) were made during late March or early April of 1999, 2001 and 2004 to capture peak snow accumulation and distribution before snowmelt. The 1999 and 2001

Table II. HRU meteorological observations summary

	Total precipitation (mm)				Mean temperature (°C)				Mean RH (%)				Mean wind speed (m s ⁻¹)			
	1998/1999	2000/2001	2003/2004		1998/1999	2000/2001	2003/2004		1998/1999	2000/2001	2003/2004		1998/1999	2000/2001	2003/2004	
UB	163	126	131		-11.5	-8.5	-9.2		80.6	77.1	80.5		4.2	5.3	4.7	
PLT	152	118	127		-11.8	-8.1	-9.2		76.6	73.4	73.7		4.2	5.3	3.7	
NF	152	118	127		-11.8	-8.1	-9.2		76.6	73.4	73.7		2.4	2.5	2.4	
SF	152	118	127		-11.3	-7.7	-8.6		78.7	74.5	75.2		2.4	3.1	3.2	
VB	151	117	127		-12.6	-9	-11		79.1	81.7	85.4		2.1	1.9	1.9	

surveys spanned a distance of approximately 615 m (centre snow survey transect in Figure 1). Approximately, 160, 400 and 50 depth measurements were taken on the NF, SF and VB, respectively. Snow depth was measured every 1–2 m, while snow density was measured every 20–25th depth measurement using an ESC30 snow tube. The 2004 snow survey spanned all three transects shown in Figure 1 but did not go as far north as the 1999 and 2001 survey. Depth measurements were taken approximately every 5–10 m. Approximately 50, 50 and 10 depth measurements were taken on the NF, SF and VB, respectively. A snow survey was also performed on the PLT HRU on 12 April 2004. The PLT snow survey spanned 120 m, consisting of 25 depth measurements and 4 density measurements. To calculate mean SWE for an HRU, the mean measured snow density for a particular HRU was applied to each depth measurement in that HRU.

Blowing snow modelling methodology

PBSM with the S_R parameterizations was applied using the Cold Regions Hydrological Modelling (CRHM) platform (Pomeroy *et al.*, 2007). CRHM has a modular, object-oriented structure whereby the user specifies which physically based algorithms (known as modules) are used to simulate hydrological processes. Parameter values required by PBSM (h_v , d_v , N , fetch) are presented in Table I for each HRU. Parameter values for vegetation were established according to field observations from site visits in February 2008. Fetch distances for each HRU were computed by applying the FETCHR program (Lapen and Martz, 1993) to a 30 m × 30 m digital elevation model (DEM). Fetch, as measured by the FETCHR program, is the distance from a cell to the nearest cell that is considered to be a topographic obstacle. A topographic obstacle is defined as follows:

$$Z_{\text{test}} \geq Z_{\text{core}} + NI \quad (10)$$

where Z_{core} is the elevation of the cell for which the fetch distance is being measured, Z_{test} is the elevation of the cell tested as a topographic obstacle, N is the distance from Z_{core} to Z_{test} and I is the obstacle height increment. FETCHR performs fetch analysis in the compass directions N, NE, E, SE, S, SW, W and NW. The HRU fetch distances used in the simulations were the mean of the fetch distance measured for each cell within an HRU. For this application, $I = 15$ cm provided the mean HRU fetch distances, which seemed appropriate based on visual observations during site visits in 2008.

Wind direction and speed measurements from the UB meteorological station were used to sum u^4 values binned by direction to determine the predominant u^4 direction(s) (S_R Scheme 2) and to activate S_R changes (S_R Scheme 3). UB wind speed and direction measurements are available only for 2003/2004. To qualitatively ascertain that the predominant u^4 direction was also the same for 1998/1999 and 2000/2001, wind measurements from a nearby alpine meteorological station at a similar elevation

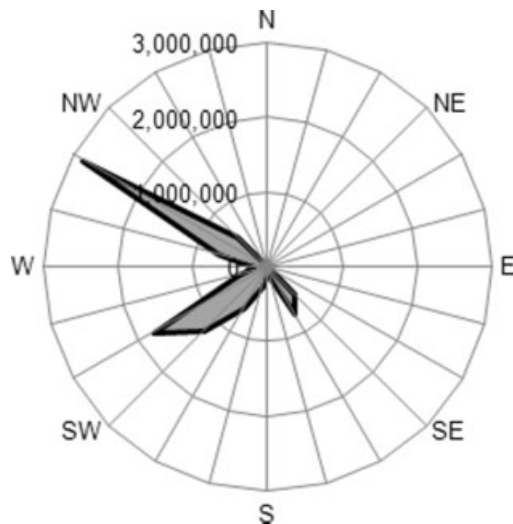


Figure 2. u^4 direction for (a) 1998/1999, (b) 2000/2001 and (c) 2003/2004. Scale is the fourth power of wind speed ($m s^{-1}$)

were examined. The predominant u^4 directions measured at this alpine station were the same for 1998/1999, 2000/2001 and 2003/2004 (southerly wind); therefore, the authors assume that the predominant u^4 directions measured at UB during 2003/2004 can also be applied to 1998/1999 and 2000/2001 simulations. Figure 2 shows the u^4 summation binned by direction for November 2003 to March 2004. There were two predominant u^4 directions measured over 2003/2004, from the northwest and from the southwest (Figure 2).

Interface lengths d_i were drawn manually and measured on the 30 m \times 30 m DEM and are presented on Figure 3 for S_R Scheme 2 for a southwest predominant u^4 direction. For a northwest predominant u^4 , all snow transport from UB and PLT is blown out of the basin ($S_{R,basin\ loss} = 1.0$). S_R values used for Scheme 2 are the average of the northwest- and southwest-derived values. For S_R Schemes 1 and 2, the average of the computed fetch distances for the NW and SW directions was used. For S_R Scheme 3, the fetch distance varied according to the eight binned wind directions.

By applying PBSM in point mode over each HRU, it was determined that UB and PLT are the snow transport source HRUs and NF, SF and VB are the sink HRUs. The resulting values for the three S_R schemes are presented in Table III. For S_R Scheme 1, all S_R s (including $S_{R,basin\ loss}$) are equivalent (Table IIIa). For S_R Scheme 2, the average of S_R s determined for NW and SW winds was used (Table IIIb). For S_R Scheme 3, S_R s were different for each of the eight binned wind directions (Table IIIc). For S_R Schemes 2 and 3, since UB and PLT are snow transport sources and the snow transport is fully developed across UB and PLT, $S_{R,PLT} = 0$. $L_{C,NF}$ calculated using Equation (9) was applied to d_{NF} to quantify NF and VB S_R values. The length of NF in the northeast–southwest direction L was measured to be approximately 205 m on the DEM, which for Equation (9) yields $L_{C,NF} = 0.81$. It was assumed, therefore, that 19% of the snow that was transported

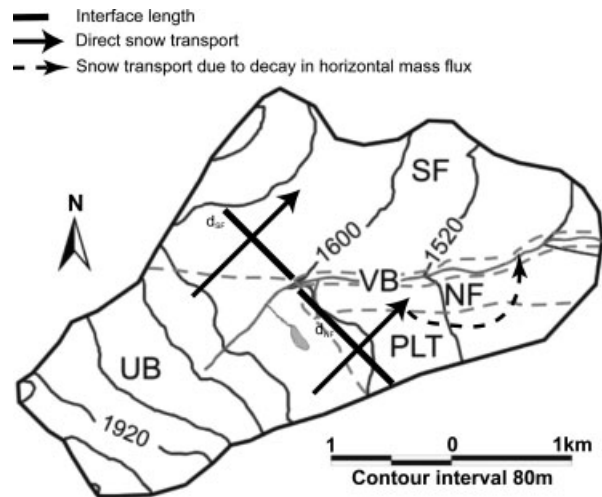


Figure 3. Granger Basin interface lengths (d) for S_R Scheme 2 (Southwest wind)

to the NF was transported further to the VB. Thus, $S_{R,NF}$ was calculated using Equation (8a) and $S_{R,VB}$ was calculated using Equation (8b) with $(1 - L_{C,NF})$. $S_{R,SF}$ was calculated using Equation (8a) with $L_{C,SF} = 1.0$.

The use of interface lengths to parameterize GB S_R values is suitable because quantities of snow transport are similar upwind from different interface lengths. For

Table III. Snow redistribution allocation factors for (a) S_R Scheme 1, (b) S_R Scheme 2, and (c) S_R Scheme 3

a)						
S_R						
UB ^a	PLT	NF	SF	VB	Loss	
1.0	0.20	0.20	0.20	0.20	0.20	
b)						
S_R						
UB ^a	PLT	NF	SF	VB	Loss	
1.0	0.00	0.28	0.16	0.06	0.50	
c)						
S_R						
Wind direction	UB ^a	PLT	NF	SF	VB	Loss
North	0.47	0.00	0.00	0.00	0.00	1.00
Northeast	0.00	0.00	0.00	0.00	0.00	1.00
East	1.00	0.00	0.00	0.00	0.00	1.00
Southeast	1.00	0.00	0.35	0.22	0.08	0.35
South	1.00	0.00	0.41	0.28	0.09	0.22
Southwest	1.00	0.00	0.51	0.37	0.12	0.00
West	1.00	0.00	0.12	0.00	0.06	0.82
Northwest	0.50	0.00	0.00	0.00	0.00	1.00

^a The S_R value for UB controls the amount of snow blown into the UB from outside Granger Basin. See text for details.

instance, consider Figure 3 and the interface lengths d_{SF} and d_{NF} . In reality, the UB fetch distance is greater upwind d_{SF} than it is upwind d_{NF} . However, once the PLT snow transport is also considered, there is similar snow transport per unit width across both d_{SF} and d_{NF} . Thus, the interface lengths alone are able to consolidate the different quantities of snow transported across d_{SF} and d_{NF} .

An apparent mismatch of scales must be addressed, with respect to the locations of the snow survey transects that are used to characterize snow conditions across the entire HRU in which they lie. Of particular concern is the location and extent of the SF transect, which was located near the eastern end of the SF HRU. Applying either S_R scheme results in snow being transported into the SF HRU. Modelling results presented in this paper show that the UB is the source of most of the blown snow deposited into the SF. This transported snow would be deposited over the western portion of the SF. As a result, it is anticipated that the simulated SF mean SWE may exceed the observed SWE.

Model evaluation

Simulated snow accumulation was evaluated using a modified Nash–Sutcliffe efficiency coefficient (MNS; Nash and Sutcliffe, 1970), the model bias (MB) and the root mean squared error (RMSE), given by

$$MNS = 1 - \frac{\sum \alpha (SWE_{sim} - SWE_{obs})^2}{\sum \alpha (SWE_{obs} - P)^2} \quad (11)$$

$$MB = \frac{\sum \alpha SWE_{sim}}{\sum \alpha SWE_{obs}} - 1 \quad (12)$$

$$RMSE = \sqrt{\frac{\sum (\alpha SWE_{sim} - \alpha SWE_{obs})^2}{n}} \quad (13)$$

where SWE_{sim} and SWE_{obs} are the simulated and observed SWE, respectively. α is the fractional area of a HRU. α is included to give greater weight to the simulated error of relatively large HRUs. n is the number of HRUs used to evaluate the RMSE. A MNS equal to 1 indicates perfectly simulated SWE. A MNS equal to zero indicates that simulated SWE is as accurate as using accumulated snowfall only (i.e. not using a blowing snow model). A positive MB indicates that SWE is overestimated. A negative MB indicates that SWE

is underestimated. The RMSE gives the average magnitude of the error in simulated snow accumulation in mm SWE.

RESULTS AND DISCUSSION

S_R scheme results

Figure 4 shows mean measured and simulated snow accumulation for the NF, SF, VB and PLT (2004 only) for (a) 17 March 1999, (b) 3 April 2001 and (c) 15 April 2004, using S_R Scheme 1. The horizontal dashed lines represent total precipitation over the simulation period. Simulated NF, SF and VB snow accumulation exceeded total precipitation in each simulation period, whereas simulated PLT snow accumulation was below total precipitation in 2004. Model performance with S_R Scheme 1 is considered inadequate, suggesting the assumption that all HRUs receive the same snow transport is not met. However, MNS scores are greater than zero (Table IV), suggesting that the model with this simple redistribution parameterization performed better than a model without consideration of blowing snow. Poor model performance is best demonstrated by the considerably overestimated VB snow accumulation and underestimated NF snow accumulation in 1999 and 2001 (Figure 4). It is noted that NF snow accumulation was closely simulated in 2004, suggesting that either the predominant u^4 direction was different over 2003/2004 than the other simulation periods, and/or differences in snow survey transects from year to year.

Figure 5 shows mean measured and simulated snow accumulation for the NF, SF, VB and PLT (2004 only) for (a) 17 March 1999, (b) 3 April 2001 and (c) 15 April 2004, using S_R Scheme 2. The horizontal dashed lines represent cumulative precipitation over the simulation period. All simulated snow accumulation fell within $\pm 1/2$ standard deviation of observed SWE except for VB in 2001. Model performance with S_R Scheme 2 is considered good for 1998/1999 and 2000/20001 and excellent for 2003/2004. This suggests that redistributing snow with regard to predominant seasonal wind direction as well as the spatial arrangement, topography and vegetation of HRUs can be successful in estimating snow accumulation. As for model performance using S_R Scheme 1, there was considerable divergence between 1998/1999 and 2000/2001, and 2003/2004 results.

Figure 6 shows mean measured and simulated snow accumulation for the NF, SF, VB and PLT for 15 April 2004, using S_R Scheme 3. The horizontal dashed line

Table IV. Modified Nash–Sutcliffe efficiency coefficient, model bias and root mean squared error for simulated snow accumulation

S_R Scheme	Modified Nash–Sutcliffe coefficient			Model bias			Root mean squared error		
	1999	2001	2004	1999	2001	2004	1999	2001	2004
1	0.42	0.47	0.04	0.03	0.12	0.02	3.7	6.2	3.0
2	0.66	0.68	0.98	0.00	0.08	0.02	3.0	5.4	0.5
3	—	—	0.85	—	—	−0.05	—	—	1.3

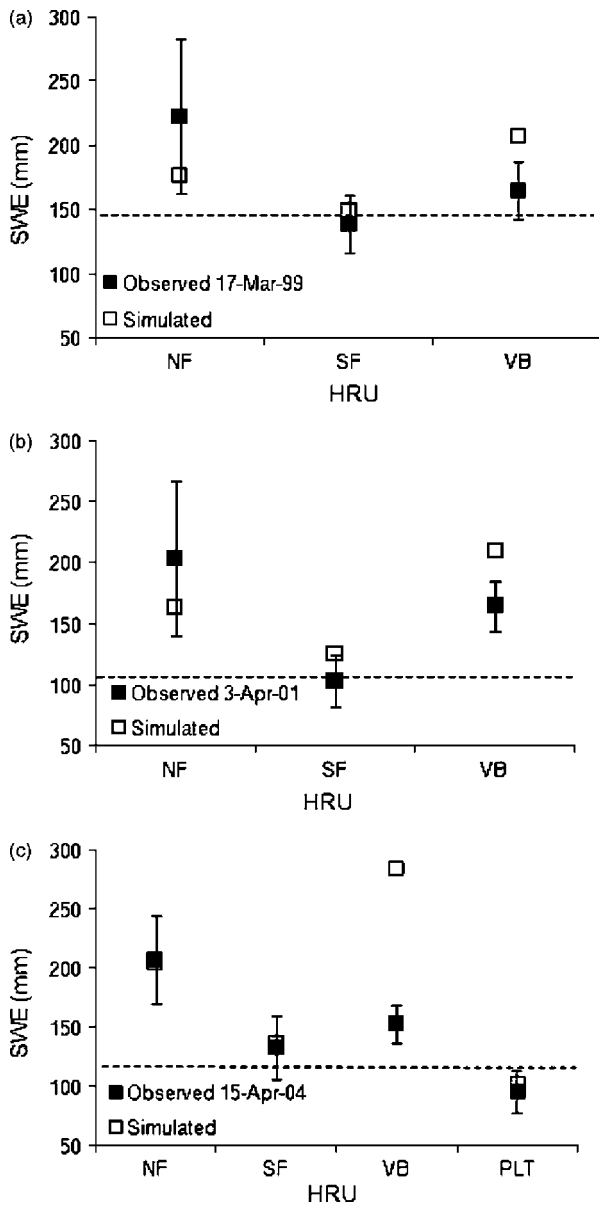


Figure 4. Measured and simulated snow accumulation using S_R Scheme 1 for the NF, SF and VB for (a) 17 March 1999, (b) 3 April 2001 and (c) 15 April 2004. $\pm 1/2$ standard deviation of observed SWE is included. Dashed line represents cumulative snowfall

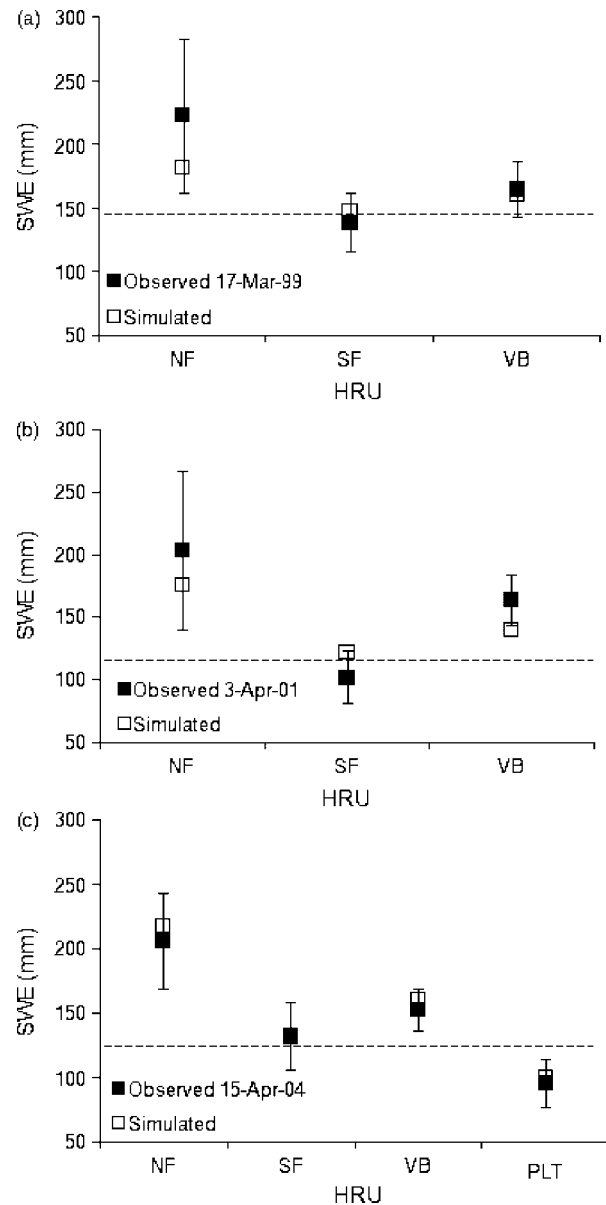


Figure 5. Measured and simulated snow accumulation using S_R scheme 2 for the NF, SF and VB for (a) 17 March 1999, (b) 3 April 2001 and (c) 15 April 2004. $\pm 1/2$ standard deviation of observed SWE is included. Dashed line represents cumulative snowfall

represents cumulative precipitation over the simulation period. All simulated snow accumulation fell within $\pm 1/2$ standard deviation of observed SWE. Model performance with S_R Scheme 2 is considered excellent for 2003/2004 (Table IV), though wind direction data for 1998/1999 and 2000/2001 could have provided additional insight and validation. This suggests that redistributing snow by blowing snow event-based wind direction, as well as the spatial arrangement, topography and vegetation of HRUs can successfully estimate snow accumulation

Comparison of different S_R schemes

Model evaluation statistics presented in Table IV show that applying PBSM with any of the S_R schemes over each simulation period provided improved simulated snow accumulation as compared to a model without

a blowing snow parameterization (all MSN >0). Even the most rudimentary snow redistribution scheme (S_R Scheme 1) improved simulated snow accumulation.

S_R Scheme 2 (defining S_R values based on a predominant u^4 direction) provided the most accurately modelled snow accumulation. It is unclear how S_R Scheme 3 would have performed over 1998/1999 and 2000/2001. In view of the S_R Scheme 2 and 3 results, it is evident that a snow redistribution parameterization that incorporates wind direction, interface lengths and snow trapping efficiency can adequately simulate snow accumulation in HRUs over complex terrains such as this mountainous sub-Arctic catchment.

Having established that S_R Scheme 2 provided good to excellent simulated snow accumulation, and that results are available for all three simulation periods, simulated snow accumulation and blowing snow sublimation

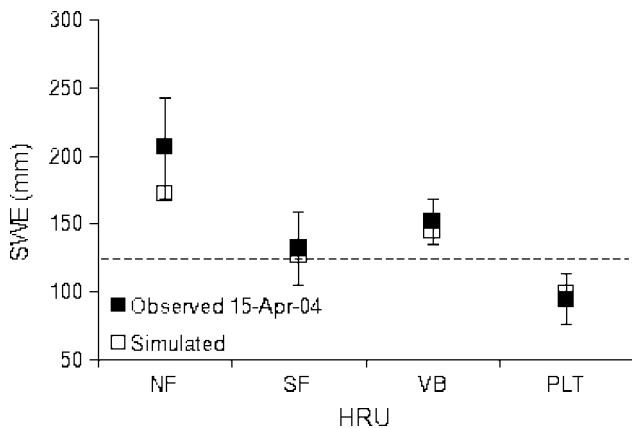


Figure 6. Measured and simulated snow accumulation using S_R Scheme 3 for the NF, SF and VB for 15 April 2004. $\pm 1/2$ standard deviation of observed SWE is included. Dashed line represents cumulative snowfall

results for UB and PLT are presented and discussed in Figure 7. This figure shows cumulative area-weighted average snowfall, simulated snow transport into UB from outside GB, simulated cumulative SWE and simulated cumulative blowing snow sublimation for the UB and PLT for (a) 1998/1999, (b) 2000/2001 and (c) 2003/2004 to the same end dates as Figures 4 and 5, using S_R Scheme 2. UB and PLT simulated snow accumulation were both less than cumulative snowfall for each simulation period, as snow was blown from these HRUs downwind. Simulated snow accumulation for the UB was 130, 12 and 50 mm for 1998/1999, 2000/2001 and 2003/2004, respectively. Simulated snow accumulation for the PLT was 84, 70 and 99 mm for 1998/1999, 2000/2001 and 2003/2004, respectively. Unfortunately snow survey data was not available for the UB and PLT for 1999 and 2001. However, surveys and aerial photography of nearby terrain in 2001 showed complete snow erosion from high exposed ridges in spring 2001. A snow survey across the east side of the PLT on 16 April 2004 (Figure 1) provided a mean SWE of 95 mm; therefore PLT cumulative SWE was well simulated for 2004. The relative amount of simulated blowing snow sublimation varied widely over each simulation period. Simulated cumulative blowing snow sublimation as a fraction of cumulative snowfall over and snow transport into UB was 19, 81 and 51% for 1999, 2001 and 2004, respectively. Simulated UB cumulative sublimation for 2001 and, in particular, 2004 was higher than is normally reported in the literature for more level environments (Pomeroy *et al.*, 1993, 1997; Pomeroy and Li, 2000; Liston and Sturm, 2002; Bowling *et al.*, 2004). Simulated cumulative blowing snow sublimation as a fraction of cumulative snowfall over PLT was 21, 23 and 9% for 1999, 2001 and 2004, respectively which corresponds well with estimates in the low-Arctic tundra (Pomeroy *et al.*, 1997; Essery *et al.*, 1999) and northern Alaska (Bowling *et al.*, 2004). Difficulties simulating UB snow accumulation and sublimation for the 2000/2001 simulation period are attributed to the high observed wind speeds and the assumption that this could

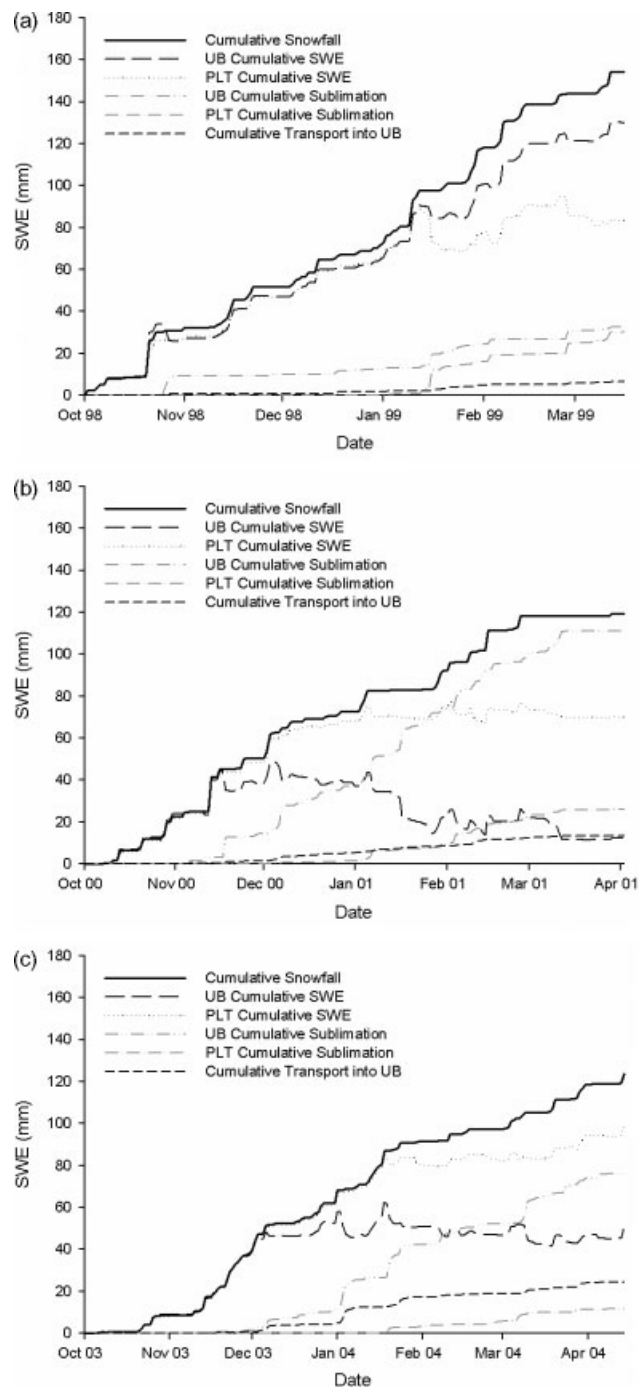


Figure 7. Average cumulative snowfall, simulated snow accumulation and cumulative sublimation for UB and PLT using S_R Scheme 2 for (a) 1998/1999, (b) 2000/2001 and (c) 2003/2004

be evenly applied uniformly to irregular high alpine terrain. The UB wind speed itself is considered realistic and during 2000/2001 was on average 1.1 m s^{-1} faster than during 1998/1999 (Table II). UB wind speed measurements were less right-skewed during 2000/2001 than during 1998/1999 (skewness of 0.9 vs 1.4). The higher mean wind speed and greater proportion of higher wind speed measurements during 2000/2001 cause the blowing snow model to almost completely ablate the UB snowpack, as the low UB roughness element density and height were unable to retain a snowpack under such wind

regimes. It is possible that breaking the UB HRU into an exposed and a sheltered HRU would reduce the very high erosion and sublimation rates modelled over this season and permit greater snow retention in the UB during high wind speed winters. However, it should be noted that nearly complete ablation of snow by wind was observed over much of the UB in 2001.

Topographic and vegetative controls

PBSM was applied over GB using S_R Scheme 2 to evaluate the independent effects of topography and vegetation on blowing snow simulations. Three modelling scenarios were used:

1. inclusion of both topography and vegetation (results presented above);
2. inclusion of vegetation only;
3. inclusion of topography only.

Vegetation protruding above a snowpack acts as roughness elements that partition the shear stress imparted by the wind flow, thus reducing scouring of the snowpack. The presence of irregular topography also influences the wind flow regime. In general, wind speed is reduced on leeward surfaces (e.g. NF) and topographic depressions (e.g. VB) as compared to flat and windward surface. Scenario 1 is as presented above and discussed for results shown in Figure 5 and Table IV. For scenario 2, the vegetation height and density of each HRU were set to zero to eliminate the modelled aerodynamic effects of vegetation. Each HRU was driven by the same meteorological observations as for scenario 1. For scenario 3, all HRUs were made flat, set to the same elevation and driven by the PLT meteorological observations. HRU vegetation height and density were retained as per scenario 1.

Figure 8 shows the corroboration of measured and simulated snow accumulation for 1998/1999, 2000/2001 and 2003/2004 using S_R Scheme 2 for (a) inclusion of both topography and vegetation, (b) vegetation only, and (c) topography only. MNS, MB, RMSE as well as coefficient of determination (R^2) and slope of corroboration (Slope) are presented on Figure 8. A value of $R^2 = 1.0$ indicates perfect corroboration of simulated and measured snow accumulation, though R^2 does not reflect simulated bias. A slope < 1.0 indicates that snow accumulation is generally underestimated, whereas a slope > 1.0 indicates that snow accumulation is generally overestimated. Including both topography and vegetation (scenario 1) provided the best simulated snow accumulation (Figure 8a). Simulated snow accumulation over Granger Basin when including vegetation but omitting topography (scenario 2) was similar to simulated snow accumulation when including both topography and vegetation (scenario 1), though the model statistics were generally not as good, particularly the MNS and slope. Topography exerts a strong control on NF drift accumulation as demonstrated by the good NF results using scenario 3 and poorer NF results using scenario 2. When vegetation was omitted

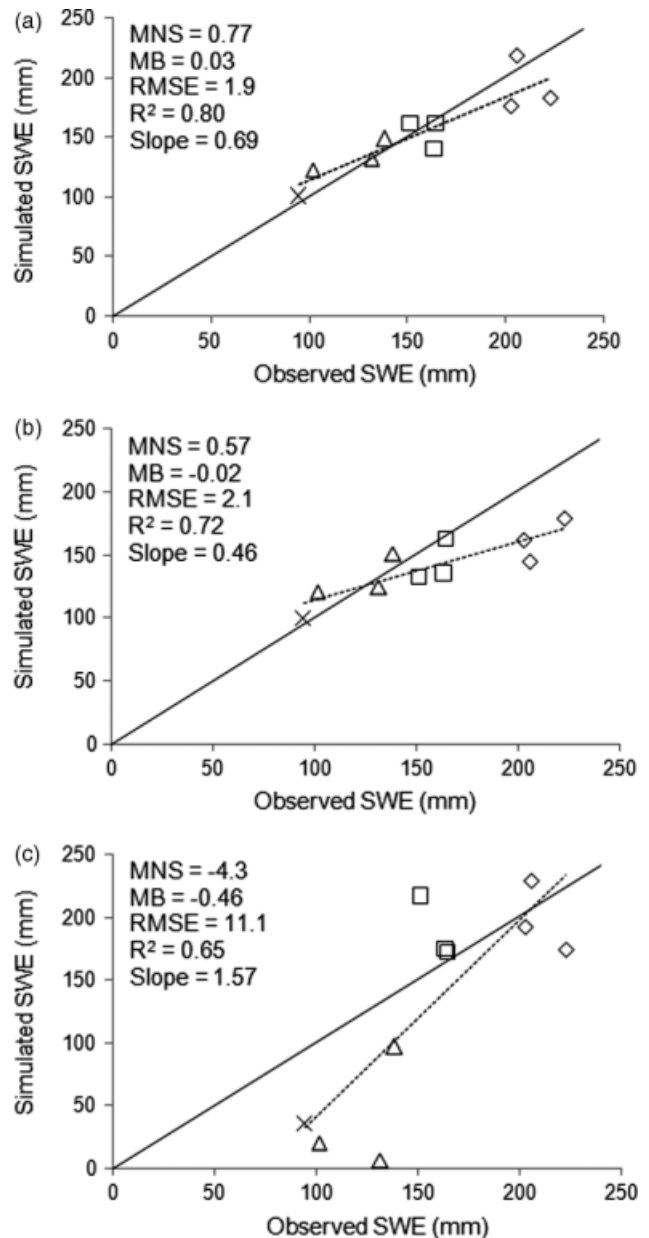


Figure 8. Corroboration of measured and simulated snow accumulation for all of 1998/1999, 2000/2001 and 2003/2004 using S_R Scheme 2 for (a) inclusion of both topography and vegetation, (b) inclusion of vegetation only, and (c) inclusion of topography only. Solid line = 1:1 corroboration. \diamond = NF, \triangle = SF, \square = VB, \times = PLT

(scenario 3), snow accumulation was considerably underestimated for the SF, indicating that vegetation has a strong control on SF snow accumulation by preventing scouring of the snowpack.

The MNS, MB and RMSE model evaluation statistics are weighted by HRU area; consequently more model error is attributed to the SF HRU. As a result, simulated snow accumulation over GB is more strongly dependent on an explicit model representation of landscape vegetation than on topography since SF simulated snow accumulation was so poor using scenario 3. It is, however, less clear whether this stronger dependence on vegetation can be generalized to other locations with similar topographic and vegetative features. The

model statistics presented in Figure 8 strongly suggests that both vegetation and topography need to be represented in order to most confidently simulate the winter evolution of SWE. This is important not only for the winter surface energy balance and snowpack energetics but also for ecology and human uses of the winter environment.

CONCLUSIONS

This study has shown that end-of-winter snow accumulation can be modelled over mountainous sub-Arctic terrain using a physically based blowing snow model. Snow accumulation and redistribution were modelled using a blowing snow model developed for prairie landscapes with minor modifications to account for the difference in partitioning of the wind shear stress due to the geometry and density of tundra shrubs compared to that due to crop stalks.

Snow transport fluxes were distributed across a catchment demarcated by multiple HRUs using the inter-HRU snow redistribution allocation factors S_R . Three S_R schemes of varying complexity were evaluated. Even the most rudimentary snow redistribution scheme improved simulated snow accumulation when compared to a model without any blowing snow parameterization. Model results show that end-of-winter snow accumulation can be accurately simulated using a physically based blowing snow model when S_R values are established that take into account wind direction and speed, HRU slope and aspect, along with the spatial arrangement of the HRUs in the catchment.

Snow accumulation was best simulated by including explicit representations of both landscape vegetation and topography, though simulated snow accumulation was more strongly dependent on vegetation cover than on topography over GB. It is, however, less clear whether this stronger dependence on vegetation can be generalized to other locations with similar topographic and vegetative features.

It appears that a similar level of representation of landscape heterogeneity is required for modelling both the snow accumulation and ablation periods, as the HRUs used here corresponded well with those for the ablation period demonstrated by Dornes *et al.* (2008a,b), demonstrating self-similarity in the landscape characteristics that govern snow accumulation, redistribution and ablation.

Future work will involve examining the utility of physically based windflow models to estimate topographically varied wind speed over mountainous catchments. This work will be valuable for hydrological predictions in poorly gauged and ungauged basins.

ACKNOWLEDGEMENTS

The authors would like to acknowledge Dell Bayne, Raoul Granger, Newell Hedstrom and Brenda Toth (Environment Canada), Rick Janowicz and Glen Carpenter

(Yukon Environment), Richard Essery (University of Edinburgh), Susanne Hanson (Danish National Space Centre), Dan Bewley and Natasha Neumann (University of British Columbia); Tim Link (University of Idaho), Michael Solohub (University of Saskatchewan) and Jean Emmanuel Sicart (Université Montpellier) for WCRB research site operations, field observations, instrument deployment and data QA/QC. The financial support of Environment Canada-MAGS, UK-NERC, Welsh Assembly Government, USA-NOAA-GAPP, CFCAS-IP3 Network, IPY Canadian Fund, NSERC Discovery Grants and the Canada Research Chair Programme is gratefully acknowledged. The comments made by two anonymous reviews are greatly appreciated.

REFERENCES

- Anderton SP, White SM, Alvera B. 2002. Micro-scale spatial variability and the timing of snow melt runoff in a high mountain catchment. *Journal of Hydrology* **1–4**: 158–176.
- Auld H. 1995. Dependence of ground snow loads on elevation in western Canada, *Proceedings of the 63rd Western Snow Conference* **63**: 143–146.
- Bowling LC, Pomeroy JW, Lettenmaier DP. 2004. Parameterization of blowing snow sublimation in a macroscale hydrology model. *Journal of Hydrometeorology* **5**: 745–762.
- Carey SK, Quinton WL. 2004. Evaluating snowmelt runoff generation in a discontinuous permafrost catchment using stable isotope, hydrochemical and hydrometric data. *Nordic Hydrology* **35**: 309–324.
- Davidson B, Pohl S, Dornes P, Marsh P, Pietroniro A, MacKay M. 2006. Characterizing snowmelt variability in a land-surface-hydrological model. *Atmosphere-Ocean* **44**: 271–287.
- Déry SJ, Crow WT, Stieglitz M, Wood EF. 2004. Modeling snow-cover heterogeneity over complex arctic terrain for regional and global climate models. *Journal of Hydrometeorology* **5**: 33–48.
- Dornes PF, Pomeroy JW, Pietroniro A, Carey SK, Quinton WL. 2008a. Influence of landscape aggregation in modelling snow-cover ablation and snowmelt runoff in a subarctic mountainous environment. *Hydrological Sciences Journal* **53**: 725–740.
- Dornes PF, Pomeroy JW, Pietroniro A, Verseghy DL. 2008b. Effects of spatial aggregation of initial conditions and forcing data on modeling snowmelt using a land surface scheme. *Journal of Hydrometeorology* **9**: 789–803.
- Essery R, Pomeroy J. 2004. Vegetation and topographic control of wind-blown snow distributions in distributed and aggregated simulations for an Arctic tundra basin. *Journal of Hydrometeorology* **5**: 735–744.
- Essery R, Li L, Pomeroy J. 1999. A distributed model of blowing snow over complex terrain. *Hydrological Processes* **13**: 2423–2438.
- Fang X, Pomeroy JW. 2009. Modelling blowing snow redistribution to prairie wetlands. *Hydrological Processes* **23**: 2557–2569.
- Goodison BE, Metcalfe JR, Louie PYT. 1998. Summary of country analyses and results, Annex 5.B Canada. In *The WMO Solid Precipitation Measurements Intercomparison Final Report, Instruments and Observing Methods Report No. 67*, WMO/TD 872; 105–112.
- Gordon M, Simon K, Taylor PA. 2006. On snow depth predictions with the Canadian Land Surface Scheme including a parameterization of blowing snow sublimation. *Atmosphere-Ocean* **44**: 239–255.
- Granger RJ, Gray DM, Dyck GE. 1984. Snowmelt infiltration to frozen prairie soils. *Canadian Journal of Earth Sciences* **21**: 669–677.
- Greene EM, Liston GE, Pielke RA. 1999. Simulation of above treeline snowdrift transport using a numerical snow-transport model. *Cold Regions Science and Technology* **30**: 135–144.
- Hasholt B, Liston GE, Knudsen NT. 2003. Snow-distribution modelling in the Ammassalik Region, South East Greenland. *Nordic Hydrology* **34**: 1–16.
- Hiemstra CA, Liston GE, Reiners WA. 2002. Snow redistribution by wind an interactions with vegetation at upper treeline in the Medicine Bow Mountains, Wyoming, U.S.A. *Arctic, Antarctic, and Alpine Research* **34**: 26–273.

- Lapen DR, Martz LW. 1993. The measurement of two simple topographic indices of wind sheltering-exposure from raster digital elevation models. *Computers & Geosciences* **19**: 769–779.
- Lettau H. 1969. Note on aerodynamic roughness-parameter estimation on the basis of roughness element description. *Journal of Applied Meteorology* **8**: 828–832.
- Li L, Pomeroy JW. 1997. Estimates of threshold wind speeds for snow transport using meteorological data. *Journal of Applied Meteorology* **36**: 205–213.
- Liston GE, Sturm M. 1998. A snow transport model for complex terrain. *Journal of Glaciology* **44**: 498–516.
- Liston GE, Sturm M. 2002. Winter precipitation patterns in arctic Alaska determined from a blowing-snow model and snow-depth observation. *Journal of Hydrometeorology* **3**: 646–659.
- Luce CH, Tarboton DG, Cooley KR. 1998. The influence of the spatial distribution of snow on basin-averaged snowmelt. *Hydrological Processes* **12**: 1671–1683.
- McCartney SE, Carey SK, Pomeroy JW. 2006. Intra-basin variability of snowmelt water balanced calculations in a subarctic catchment. *Hydrological Processes* **20**: 1001–1016.
- Nash JE, Sutcliffe JV. 1970. River flow forecasting through conceptual model. Part 1—a discussion of principles. *Journal of Hydrology* **10**: 282–290.
- Pomeroy JW. 1989. A process-based model of snow drifting. *Annals of Glaciology* **13**: 237–240.
- Pomeroy JW. 1991. Transport and sublimation of snow in wind-scoured alpine terrain. In *Snow, Hydrology and Forests in Alpine Areas, International Association of Hydrological Sciences Publication No. 205*, Bergman H, Lang H, Frey W, Issler D, Salm B (eds). IAHS Press: Wallingford; 131–140.
- Pomeroy JW, Bewley DS, Essery RLH, Hedstrom NR, Link T, Granger RJ, Sicart JE, Ellis CR, Janowicz JR. 2006. Shrub tundra snowmelt. *Hydrological Processes* **20**: 923–941.
- Pomeroy JW, Gray DM. 1990. Saltation of snow. *Water Resources Research* **26**: 1583–1594.
- Pomeroy JW, Gray DM, Brown T, Hedstrom NR, Quinton W, Granger RJ, Carey SK. 2007. The cold regions hydrological model: a platform for basing process representation and model structure on physical evidence. *Hydrological Processes* **21**: 2650–2667.
- Pomeroy JW, Gray DM, Landine PG. 1991. Modelling the transport and sublimation of blowing snow on the prairies. *Proceedings of the Eastern Snow Conference* **48**: 175–188.
- Pomeroy JW, Gray DM, Landine PG. 1993. The Prairie Blowing Snow Model: characteristics, validation and operation. *Journal of Hydrology* **144**: 165–192.
- Pomeroy JW, Hedstrom N, Parviainen J. 1999. The snow mass balance of Wolf Creek: effects of snow, sublimation and redistribution. In *Wolf Creek Research Basin: Hydrology, Ecology, Environment*, Pomeroy JW, Granger R (eds). Environment Canada: Saskatoon; 15–30.
- Pomeroy JW, Li L. 2000. Prairie and arctic areal snow cover mass balance using a blowing snow model. *Journal of Geophysical Research-Atmospheres* **105**: 26619–26634.
- Pomeroy JW, Male DH. 1986. Physical modelling of blowing snow for agricultural production. In *Proceedings, Snow Management for Agriculture Symposium, Great Plains Agricultural Council Publication No. 120*, Steppuhn H, Nicholaichuk W (eds). Water Studies Institute: Saskatoon; 73–108.
- Pomeroy JW, Male DH. 1992. Steady-state suspension of snow. *Journal of Hydrology* **136**: 275–301.
- Pomeroy JW, Marsh P, Gray DM. 1997. Application of a distributed blowing snow model to the Arctic. *Hydrological Processes* **11**: 1451–1464.
- Purves RS, Barton JS, Mackaness WA, Sugden DE. 1998. The development of a rule-based spatial model of wind transport and deposition of snow. *Annals of Glaciology* **26**: 197–202.
- Raupach MR, Gillette DA, Leys JF. 1993. The effect of roughness elements on wind erosion threshold. *Journal of Geophysical Research* **98**: 3023–3029.
- Takeuchi M. 1980. Vertical profile and horizontal increase of drift-snow transport. *Journal of Glaciology* **26**: 481–492.
- Winstral A, Elder K, Davis RE. 2002. Spatial snow modeling of wind-redistributed snow using terrain-based parameters. *Journal of Hydrometeorology* **3**: 524–538.
- Winstral A, Marks D. 2002. Simulating wind fields and snow redistribution using terrain-based parameters to model snow accumulation and melt over a semi-arid mountain catchment. *Hydrological Processes* **16**: 3585–3603.
- Wyatt VE, Nickling WG. 1997. Drag and shear stress partitioning in sparse desert creosote communities. *Canadian Journal of Earth Sciences* **34**: 1486–1498.